Journal of Structural Geology, Vol. 5, No. 5, pp. 539 to 548, 1983
Printed in Great Britain

0191–8141/83 $03.00 + 0.00

Randomness testing in three-dimensional orientation data

N. H. WOODCOCK

Department of Earth Sciences, Downing Street, Cambridge CB2 3EQ, U.K.

and

M. A. NAYLOR

Petroleum Development Oman, P.O. Box 81, Muscat, Sultanate of Oman

(*Received* 8 *December* 1982; *accepted in revised form* 6 *May* 1983)

Abstract—We review published methods of testing for randomness in 3D axial orientation data. We then propose a new test based on eigenvalue analysis. The test statistic is S_1/S_3, the ratio of the largest to smallest eigenvalues of the orientation tensor. Critical values of this statistic are tabulated and graphed for sample sizes between 5 and 1000, for four confidence levels. The calibrations of S_1/S_3 were performed by a Monte-Carlo sampling method. The same random samples have been assessed using other tests, as have some natural orientation data samples. We conclude that the S_1/S_3 test is easier to use and more generally applicable than previous tests, particularly for the common type of data in structural geology.

INTRODUCTION

A COMMON problem confronting the structural geologist when analysing orientation data is assessing the significance of a computed mean orientation. This difficulty arises primarily when dealing with nearly 'random' data; that is data with only a weak preferred orientation. Such data arise, for example, from sampling of fold hinges, bedding planes and fault planes in mélange terrains. Formally the question to be asked is: are the data a random sample of a uniform distribution of directions, or is there a significant preferred orientation?

Although tests for uniformity are well developed for 2D orientation data (e.g. Mardia 1972, pp. 132–137 and 173–195), there are few simple convenient tests for 3D uniformity. The existing tests have a number of disadvantages:

(1) some are parametric, in the sense that they assume that the data have a certain form or distribution;
(2) some are designed for large sample sizes; these may be acceptable in petrofabric studies but are impractical for generally less abundant field measurements;
(3) rotational variance may have to be taken into account, that is the test outcome may vary if the same data are rotated (in space or on an equal-area projection), and
(4) some tests involve tedious and time-consuming allocation of data to 'cells' on an equal-area projection, and the use of cumbersome tables to determine critical test values.

Since computer programs are now widely used in the analysis and plotting of 3D orientation data (e.g. Woodcock 1973, Nuttall & Cooper 1978, Mancktelow 1981), it is desirable and convenient to design a rapid, simple test to be used in the context of such programs. In this paper we describe a test based on the eigenvalue method of orientation data analysis (Watson 1966, Woodcock 1977), which is suitable for both large and small sample sizes.

OVERVIEW OF AVAILABLE RANDOMNESS TESTS

This review is not exhaustive, but indicates available tests commonly used, or suitable for use, by structural geologists.

Tests using cells on an equal-area net

In *Winchell's zonal test* (e.g. Chayes 1949) the equal-area net is divided into 10 concentric cells of equal area (Fig. 1a). A uniform distribution (size N) has an identical expected frequency ($=N/10$) in each cell. A χ^2 statistic can be calculated which measures deviations from uniformity, thus:

$$\chi^2 = \sum_{i=1}^{10} (E_i - O_i)^2/E_i, \qquad (1)$$

where E_i = expected frequency, O_i = observed frequency, i = cell number. This value is to be compared with the tabulated χ^2 statistic with 9 degrees of freedom. The test suffers from the disadvantage that it is not rotationally invariant; the test outcome depends on the location of the mean on the net. To obtain reproducible tests, the mean of a cluster or the pole to a girdle should first be rotated to the net centre.

Further disadvantages of the test are: (a) it is best applied to samples with at least 50 and preferably more than 100 points and (b) it is biased, finding too many distributions significant compared with other tests.

Flinn (1958) proposed a *modified Winchell test* with

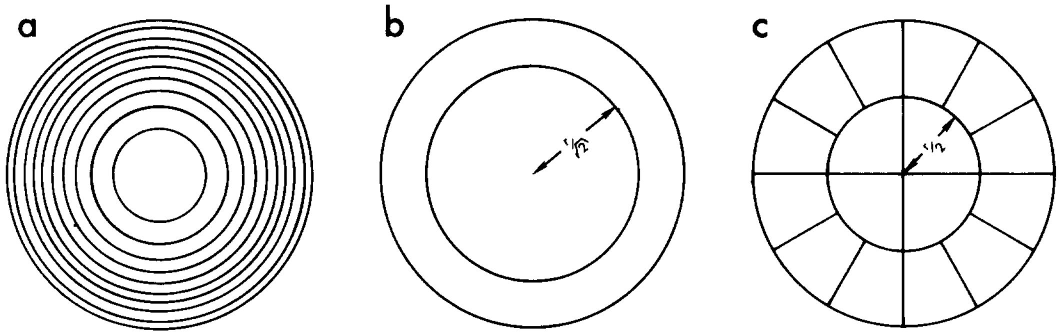

Fig. 1. Three methods of subdividing an equal-area projection for counting data: (a) 10 cells for the Winchell test, (b) 2 cells for the modified Winchell test proposed by Flinn (1958), (c) 16 cells for the tests of Dudley *et al.* (1975).

only two concentric cells of equal area (Fig. 1b). A similar χ^2 statistic can be calculated and compared with tabulated χ^2 for one degree of freedom. This simplification of the cell pattern overcomes the limitation on the number of data points to be tested, but the test is still rotationally variant and biased.

In the *Winchell general test*, a square grid is thrown over the equal-area projection of data. The grid must have approximately as many squares as the number of data points. If the sample is random, the frequency of cells with various numbers of points is given by a Poisson distribution. Compatibility of the observed and expected frequencies is again made using a χ^2 test. The test requires that the minimum number of points in a cell is 5, implying that the test is only suitable for large N. A further disadvantage is the possibility that the observed frequencies will fit a Poisson distribution without the sample being random, simply because the test does not attempt to relate the cell frequencies to the relative spatial positions of the cells (Chayes 1949).

To overcome the problem of rotational variance, Dudley *et al.* (1975) proposed a test using an equal-area projection divided into 16 cells (Fig. 1c). The number of points in each cell is counted. The maximum and minimum number of points per cell (and the number of empty cells, if the minimum is zero), are compared with tabulated significance limits. The test can be performed for most N values. The most significant result from the three tests is taken. Our trials indicate that the number of points per cell and the number of empty cells are rotationally variant. However, because the most significant result of the three tests is taken, the overall outcome of the test is not always affected. Not all the tests are applicable to very small N values, and they have the further disadvantage that the tables are somewhat complex to use.

Tests using eigenvalues

The analysis of orientation data using eigenvalue/eigenvector methods is well known and is reviewed later. The method is rotationally invariant.

Anderson & Stephens (1972) devised tests for distinguishing a random sample of a uniform distribution from a cluster or a girdle in the data. If the largest eigenvalue S_1 exceeds a test value (Fig. 2a) a preferred orientation in the form of a cluster exists. Similarly, if the smallest eigenvalue S_3 is less than a critical value (Fig. 2b) there is a preferred orientation in the form of a girdle. The test values were estimated by Monte-Carlo methods, and for $N > 100$ are approximately given by

$$S_1 = 1/3 + b/\sqrt{N} \qquad (2)$$

$$S_3 = 1/3 - b/\sqrt{N}, \qquad (3)$$

where b is a constant related to the significance level. Anderson & Stephens' tabulated test values are the basis of Fig. 2.

Mardia (1972) has also proposed an eigenvalue test. Uniformity of the distribution implies $S_1 = S_2 = S_3 = 1/3$. The statistic

$$S_u = \frac{15}{2N} \sum_{i=1}^{3} (\lambda_i - N/3)^2 \qquad (4)$$

where $\lambda_i = S_i \times N$, measures deviations from uniformity. S_u values in excess of a test value (11.07 and 15.09 at the 95 and 99% confidence levels, respectively) indicate a non-random distribution. The critical values, unlike those of the Anderson & Stephens test, are independent of N.

We will follow up this promising eigenvalue approach in this paper.

Tests involving vector analysis

By treating each item of orientation data as a unit vector on the sphere, a vector sum can be found (e.g. Fisher 1953). The larger the normalised vector sum, the stronger the preferred orientation. A set of test values has been erected (Mark 1973) which can be used to test against the hypothesis of randomness. In fact S_1 and the normalized vector sum (R/N) are linearly correlated (Mark 1973)

$$S_1 = 1.24\ R/N - 0.302, \qquad (5)$$

and therefore Mark's test can be regarded as equivalent to the Anderson & Stephens S_1 test against a cluster hypothesis.

Parametric tests

It is sometimes assumed that orientation data conform to a theoretical distribution such as the Fisher (spherical

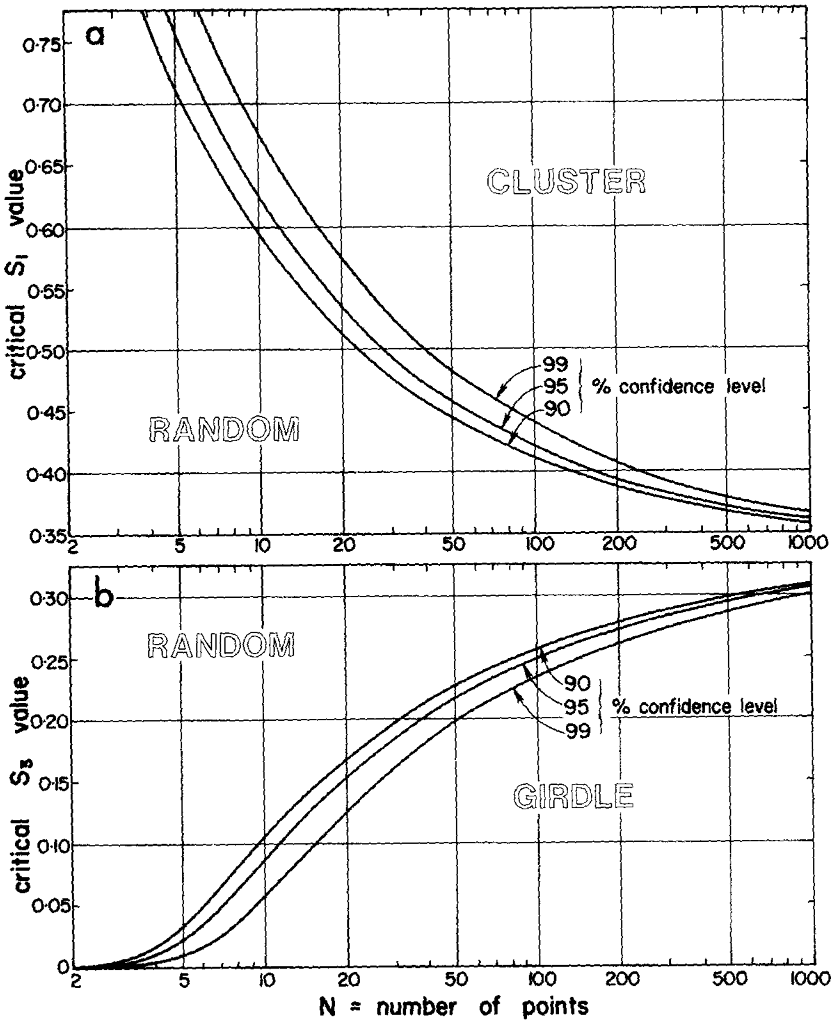

Fig. 2. Critical values for the tests of Anderson & Stephens (1972) graphed against sample size: (a) S_1 values to test for significant cluster, (b) S_3 values to test for significant girdle.

normal) distribution or the Bingham distribution. In such cases the parameters specifying the distribution can be estimated from the sample and used to test against randomness. In the case of the Fisher distribution the parameter k is a measure of the strength or dispersion of the data. Mardia (1972) gives a test based on the Bingham distribution.

Real geological data samples do not usually conform well to available ideal distributions, and the general use of this type of parametric test is likely to be misleading.

EIGENVALUE ANALYSIS OF ORIENTATION DATA

The orientation tensor method

This analytical method is the basis for both the randomness test of Anderson & Stephens (1972) and the new test proposed by us.

Individual observations are regarded as unit vectors defined by direction cosines l_i, m_i, n_i. The orientation matrix **b** is derived from the direction cosines thus

$$\mathbf{b} = \begin{bmatrix} \sum l_i^2 & \sum l_i m_i & \sum l_i n_i \\ \sum m_i l_i & \sum m_i^2 & \sum m_i n_i \\ \sum n_i l_i & \sum n_i m_i & \sum n_i^2 \end{bmatrix}. \quad (6)$$

The normalized form of this matrix $\mathbf{B} = \mathbf{b}/N$ is the *orientation tensor* of Scheidegger (1965). The eigenvectors (v_1, v_2, v_3) of this matrix correspond to three orthogonal 'principal axes' of the data sample. Axis v_1 is an estimate of the mean direction of the data; v_3 is the pole to any girdle present in the data (Watson 1966).

The eigenvectors (λ_1, λ_2, λ_3), associated with (v_1, v_2, v_3) respectively, describe the shape of the data sample (Watson 1966, Mark 1974, Woodcock 1973, 1977). Since

$$\lambda_1 + \lambda_2 + \lambda_3 = N \quad (7)$$

then normalized eigenvalues $S_j = \lambda_j/N$ are related by

$$S_1 + S_2 + S_3 = 1. \quad (8)$$

A data cluster has $S_1 > S_2 \cong S_3$ and a data girdle has $S_1 \cong S_2 > S_3$. Although the eigenvalues can be used to describe the shape of any data sample, care is needed in their detailed interpretation, particularly with multimodal data or samples with non-orthorhombic symmetry (Woodcock 1977).

The eigenvalue ratio plot

Graphical methods of further quantifying sample shapes were detailed by Woodcock (1977) and Harvey & Ferguson (1978). The most convenient graph is the Cartesian plot of S_2/S_3 (abscissa) vs S_1/S_2 (ordinate) on either linear or logarithmic axes (e.g. Wallbrecher 1979, Williams & Spray 1979). This ratio plot (Fig. 3), on which each data sample plots as a point, is in some ways analogous to the widely used 'Flinn plot' for strain ellipsoids (Flinn 1962, 1978, Cobbold & Gapais 1979, Harvey & Laxton 1980). It can similarly be divided into fields of different shape of the data sample ranging from uniaxial girdles through samples with mixed girdle and cluster attributes to uniaxial clusters (Fig. 3). This shape factor can be expressed by the gradient K of a line joining the graph origin to the point representing the sample. On the logarithmic graph this is

$$K = \ln(S_1/S_2)/\ln(S_2/S_3). \tag{9}$$

K ranges from zero (uniaxial girdles) to infinite (uniaxial clusters).

Complementary to the shape parameter is a parameter C, where

$$C = \ln(S_1/S_3) \tag{10}$$

which expresses the 'strength' of the preferred orientation in the data sample (Woodcock 1977). Strongly organized samples have larger C and plot further from the origin of the ratio graph (Fig. 3). A perfect uniform distribution of data would have $C = 0$ and would plot at the origin with $S_1 = S_2 = S_3 = 1/3$. Random samples will also plot close to the origin and have low C values, suggesting that this parameter, S_1/S_3 itself, might be used as a test statistic for randomness. This possibility is explored in this paper.

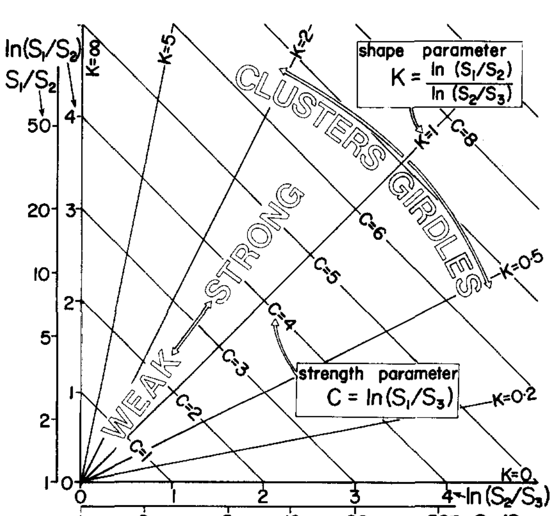

Fig. 3. The eigenvalue ratio graph for representing the shape and strength of samples of orientation data.

The most convenient way of assessing the potential of the S_1/S_3 test has been to use Monte-Carlo studies; essentially taking repeated random samples from a parent uniform distribution of directions in space. These studies, detailed below, have resulted in:

(a) the conclusion that S_1/S_3 is a natural and helpful test statistic for randomness, and
(b) development of a convenient graph of critical test values of S_1/S_3 for various sample sizes and confidence levels.

DEVELOPMENT OF THE S_1/S_3 TEST

A uniform distribution of directions

A prerequisite for our random sampling method is a reliable method for generating a 'parent' uniform distribution in space. One previous approach (e.g. Starkey 1977) has been to construct an array of points on a sphere according to the nodes of a geometric grid on the sphere surface. The grid is chosen so that for a large number of nodes the distribution approaches uniform. Every node is numbered and stored, and the array can then be sampled as necessary. We have used an alternative approach (suggested by Dr. W. H. Owens) which allows a random sample to be directly derived, without the intermediate storage of a large array representing uniformly distributed points.

By definition, a uniform distribution of directions in space projects on a sphere as an array of points that has an equal density in any area of the sphere surface, irrespective of its size or position. In particular the density of points must be the same in all spherical caps centred at one pole of the sphere (Fig. 4a). The area A of a cap extending to a plunge (i.e. latitude) $\phi°$ on a sphere of radius r is

$$A = 2\pi r^2(1 - \sin\phi). \tag{11}$$

Because we will consider only axial data, fully represented on a hemisphere, we compare the area of this cap to the total area of the hemisphere

$$A_0 = 2\pi r^2. \tag{12}$$

Hence, the area of the cap relative to that of the hemisphere is

$$A/A_0 = 1 - \sin\phi. \tag{13}$$

For a uniform density of points on a hemisphere, the number of points n in any spherical cap must also be related to the total number of points n_0 by

$$n/n_0 = 1 - \sin\phi. \tag{14}$$

We can obtain a uniform density of plunge values by sampling uniformly for n/n_0 in the range 0 to 1 and transforming to plunge using:

$$\phi = \sin^{-1}(1 - n/n_0). \tag{15}$$

This transformation is graphed in Fig. 4(b). It has the effect of shifting points away from the pole, where there

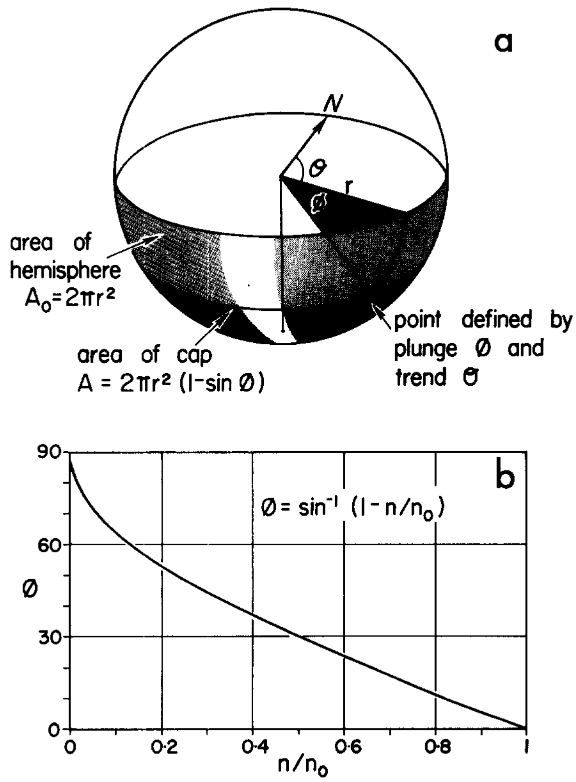

Fig. 4. Derivation of a uniform sample on a hemisphere. See text for explanation.

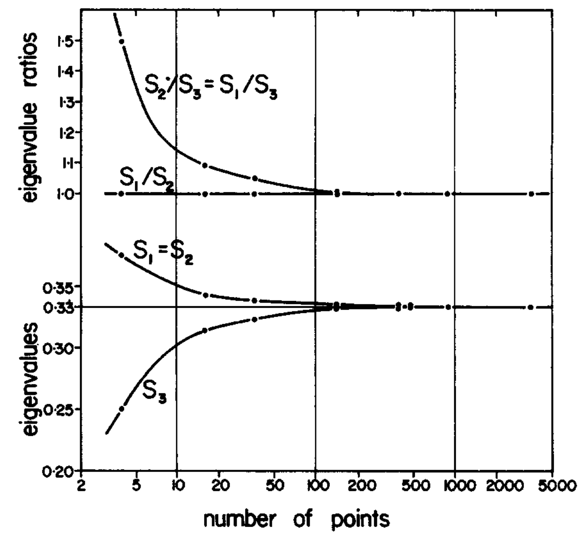

Fig. 5. Normalized eigenvalues ($S_1 + S_2 + S_3 = 1$) and eigenvalue ratios for 'uniform' samples with various numbers of points, derived using the method in Fig. 4.

would otherwise be a cluster if sampling were uniform for ϕ over the range 0–90°.

No correction is needed for trend values (θ) which can be sampled directly over the range 0–360°.

The validity of the above procedure was checked by first generating 'uniform' test samples of various sizes. The eigenvalues of these samples are shown in Fig. 5. At low sample sizes the data are clearly non-uniform, producing weak uniaxial girdles ($S_1 = S_2$) with the chosen point grid pattern. As sample size increases however, the three eigenvalues all converge on 1/3, the theoretical value for a uniform distribution, and the eigenvalue ratios approach 1.0. These results give confidence in the validity of the sampling procedure, though we must emphasize that our random sampling method does not depend on producing a perfectly uniform parent sample.

Sampling procedure

Each sample is produced directly by random sampling of the parameters θ (from 0 to 360°) and n/n_0 (from 0 to 1), with transformation of n/n_0 to ϕ by equation (15) above. A FORTRAN subroutine RANSAM performs this procedure using the random number generator provided by the CAMLIB library on the University of Cambridge IBM 3081 computer. RANSAM is the heart of a larger program RANSACK which provides the following output for each sample:

(a) eigenvectors and eigenvalue parameters and
(b) results of tests on the sample using the methods of Winchell, Dudley *et al.*, Mardia and Anderson & Stephens.

Listings of the RANSACK program are available from us.

Our Monte-Carlo sampling plan was designed to produce usable critical values of the S_1/S_3 statistic for the range of sample sizes commonly used in field geology. We chose sample sizes (N) of 5, 10, 20, 50, 100, 200, 500 and 1000 points, and took 1000 samples of each size. This number was determined by the available computing resources, but has resulted in an accuracy of the S_1/S_3 estimates which is more than adequate for most applications.

Characteristics of the Monte-Carlo samples

The main characteristics of the 1000 samples of each sample size (N) can be represented on an eigenvalue ratio graph (S_1/S_2 vs S_2/S_3) and on histograms of the 'strength' parameter (S_1/S_3) and 'shape' parameter (K). Typical examples of these plots for $N = 50$ are shown in Fig. 6. The variation with N of the mean, standard deviation and skewness of the sampling distributions for ln (S_1/S_3) and ln K is shown in Fig. 7.

The random samples have shapes which range across the complete spectrum from uniaxial girdles (zero K) to uniaxial clusters (infinite K). The average shape is close to $K = 1$, and ln K is distributed symmetrically about this value (skewness $\cong 0$, Fig. 7a). The standard deviation of ln K is rather similar ($\cong 1.0$) for different N, corresponding to 1° bounds of $K = 0.368$ and 2.72. There is a very small tendency for the mean shapes to be on the girdle side of $K = 1$, more marked at low N, and for the skewness to be negative (i.e. a tail in the cluster field). These minor effects must be attributed to the sampling procedure. They are small enough to be ignored.

Unlike the shapes of the samples, their strengths, measured by S_1/S_3, are strongly dependent on sample size N (Fig. 7b). Both the mean and standard deviation of the ln (S_1/S_3) distributions decrease with increasing

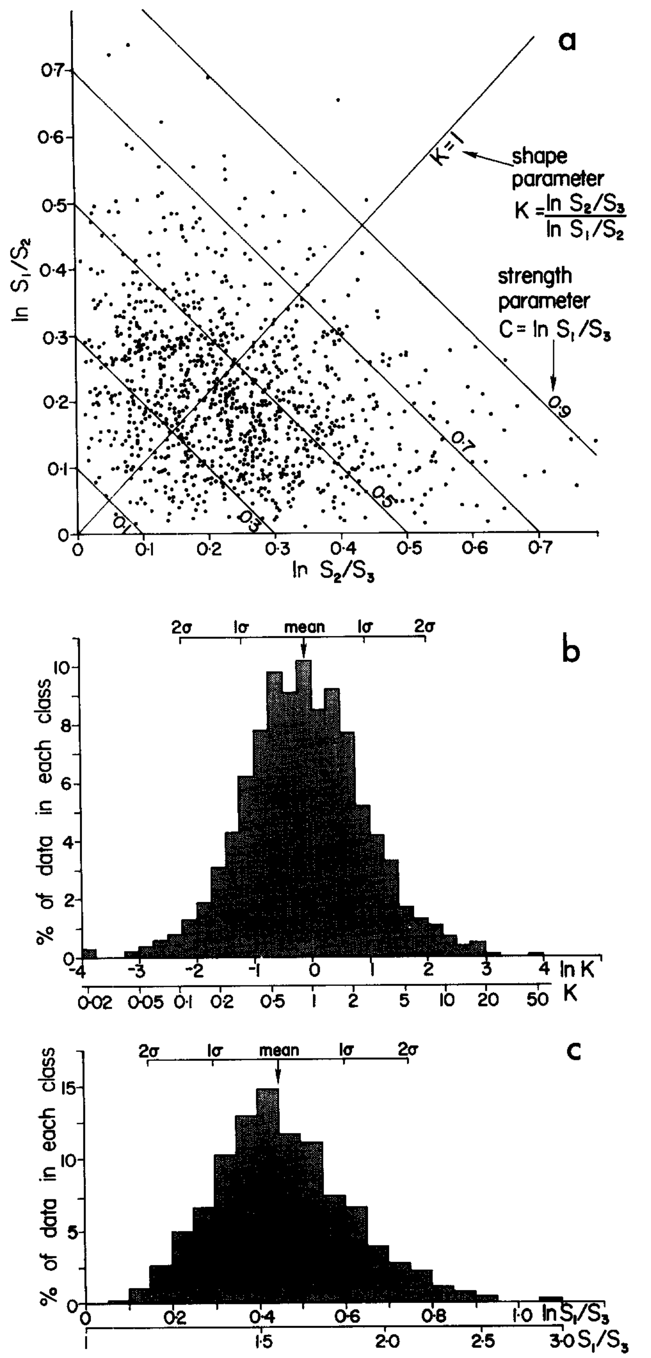

Fig. 6. Characteristics of 1000 Monte-Carlo samples each of 50 points. (a) An eigenvalue ratio plot, (b) a histogram of the shape parameter $K = \ln (S_2/S_3)/\ln (S_1/S_2)$, (c) a histogram of the strength parameter $C = \ln (S_1/S_3)$.

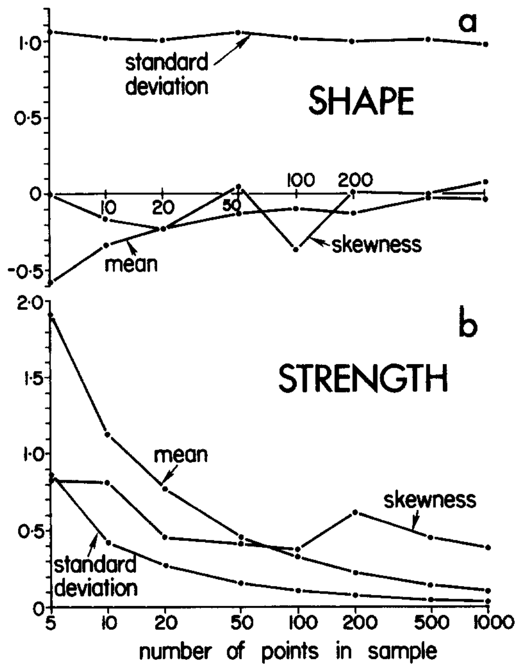

Fig. 7. Variation with sample size of the mean, standard deviation and skewness of the sampling distributions for (a) shape parameter (ln K) and (b) strength parameter (ln S_1/S_3). Examples of the sampling distributions are shown as histograms in Fig. 6.

N. In other words, the larger random samples plot closer to the origin of the eigenvalue ratio graph.

An important feature of the ratio graphs (e.g. Fig. 6a) is the tendency of the S_1/S_3 lines to form natural density contours for the point scatter. This suggests that S_1/S_3 is a rather natural measure of sample strength and therefore of randomness.

Derivation of critical S_1/S_3 *values*

To derive critical test values of the S_1/S_3 statistic we must focus on the positive tail of histograms such as that in Fig. 6(c). We can say with 99% confidence that an unknown sample (in this case with $N = 50$) is a random sample of a uniform distribution if it has S_1/S_3 less than about 2.35, the value that just includes 99% of samples on Fig. 6(c).

Critical S_1/S_3 values have been estimated in a similar way for all other sample sizes and graphed for confidence levels of 90%, 95%, 97.5% and 99% (Fig. 9). In practice, each critical value was interpolated from the best-fit curve to a cumulative plot of the ln (S_1/S_3) data (Fig. 8). The tails of these distributions on probability paper approximate to straight lines.

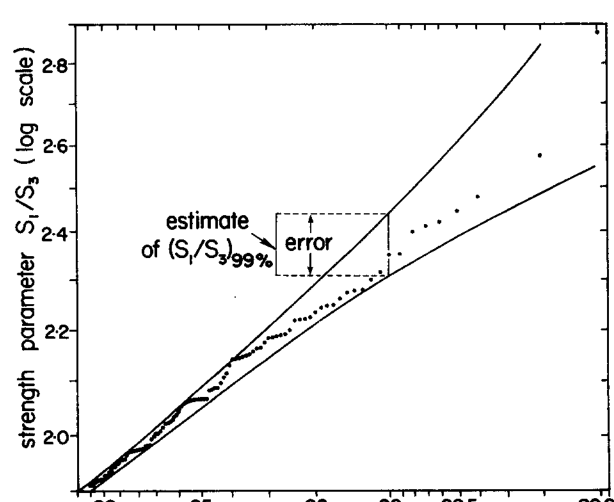

Fig. 8. Cumulative probability plot of the upper tail of the ln (S_1/S_3) histogram in Fig. 6(c), showing the method of estimating a critical S_1/S_3 value and its error.

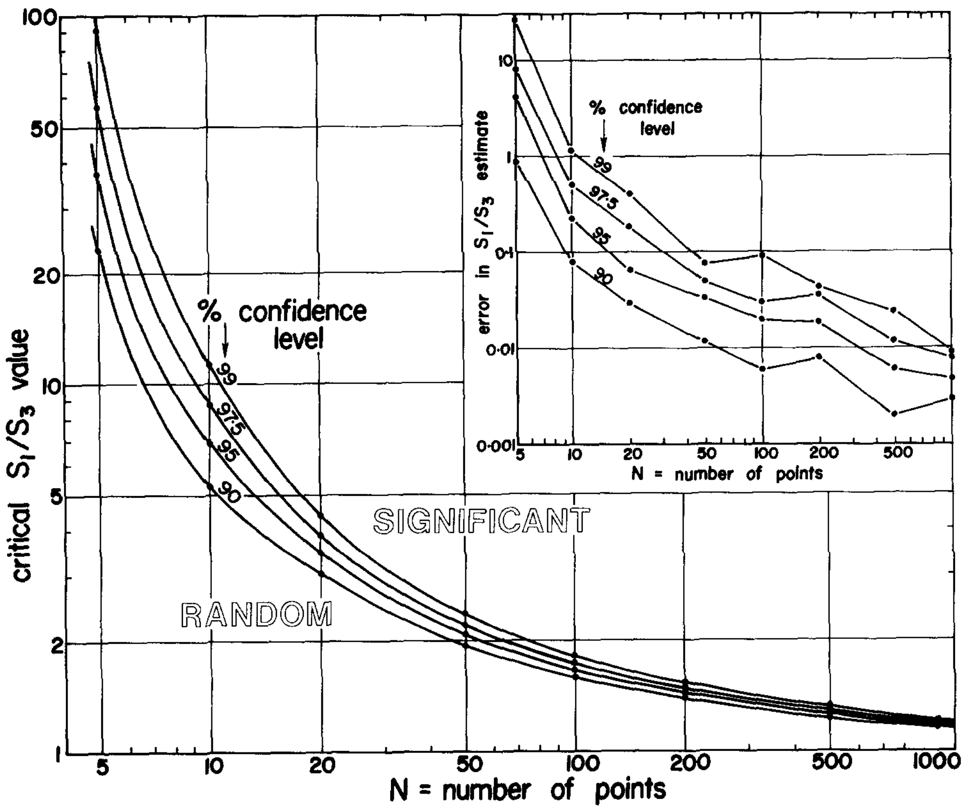

Fig. 9. Variation in the critical value of S_1/S_3 with sample size, for varying confidence levels. Inset shows the variation in the total errors, measured as shown in Fig. 8.

N	CONFIDENCE LEVEL 90%	95%	97.5%	99%	Approx. error
5	**23.1**	**37.4**	**56.7**	**91**	
6	12.0	18.5	27.5	45	10.0
7	8.9	12.5	18.5	27.5	
8	7.1	9.7	13.5	19.0	
9	6.1	8.0	10.4	14.2	
10	**5.30**	**6.83**	**8.8**	**11.3**	
12	4.50	5.55	6.6	8.2	1.0
14	3.95	5.71	5.5	6.5	
16	3.56	4.17	4.75	5.55	
18	3.27	3.80	4.25	4.89	
20	**3.037**	**3.47**	**3.89**	**4.39**	
25	2.66	2.97	3.26	3.62	
30	2.40	2.65	2.87	3.15	
40	2.09	2.28	2.44	2.61	
50	**1.923**	**2.073**	**2.21**	**2.35**	0.1
60	1.82	1.94	2.04	2.18	
70	1.73	1.83	1.93	2.05	
80	1.67	1.76	1.85	1.96	
90	1.62	1.70	1.78	1.88	
100	**1.597**	**1.667**	**1.736**	**1.82**	
120	1.52	1.58	1.64	1.73	
140	1.47	1.55	1.59	1.67	
160	1.43	1.50	1.55	1.62	
180	1.40	1.47	1.52	1.58	
200	**1.380**	**1.433**	**1.470**	**1.536**	
250	1.33	1.38	1.42	1.48	
300	1.30	1.34	1.38	1.44	
400	1.25	1.29	1.33	1.37	
500	**1.228**	**1.251**	**1.278**	**1.315**	
600	1.20	1.23	1.26	1.29	
700	1.18	1.21	1.25	1.27	
800	1.17	1.19	1.23	1.25	
900	1.16	1.18	1.21	1.23	0.01
1000	**1.161**	**1.177**	**1.192**	**1.207**	

Table 1. Critical values of the S_1/S_3 statistic for various sample sizes (N) and confidence levels

Numbers in bold face were derived directly from our Monte-Carlo tests; the remainder were interpolated from larger scale (and therefore more accurate) versions of the curves in Fig. 9. The indicated errors are only approximate. They are total errors, e.g. 1.0 indicates an error of ± 0.5 in the S_1/S_3 value.

The critical values are presented in an alternative form in Table 1, in which values for samples sizes between those in the Monte-Carlo runs have been read from the graph in Fig. 9.

The accuracy of each critical S_1/S_3 estimate was taken as the width of the envelope to the ln (S_1/S_3) data on the cumulative plot (Fig. 8). A more sophisticated approach was not thought to be justified by the amount of data available. By any assessment, the errors are rather small (Fig. 9 inset, Table 1), barely plottable on the graph of critical S_1/S_3 values (Fig. 9) except at very low sample sizes. We suggest therefore that Fig. 9 can be used with considerable confidence to assess randomness using the S_1/S_3 test.

PRACTICAL PROCEDURE FOR USING THE S_1/S_3 TEST

The following procedure is illustrated by analysis of a real data sample in Fig. 10.

(1) Express each direction in the sample as a set of three direction cosines. If the data are in the form of trend and plunge, the formulae are:

$$l = \cos(\text{plunge}) \cdot \cos(\text{trend})$$
$$m = \cos(\text{plunge}) \cdot \sin(\text{trend})$$
$$n = \sin(\text{plunge}).$$

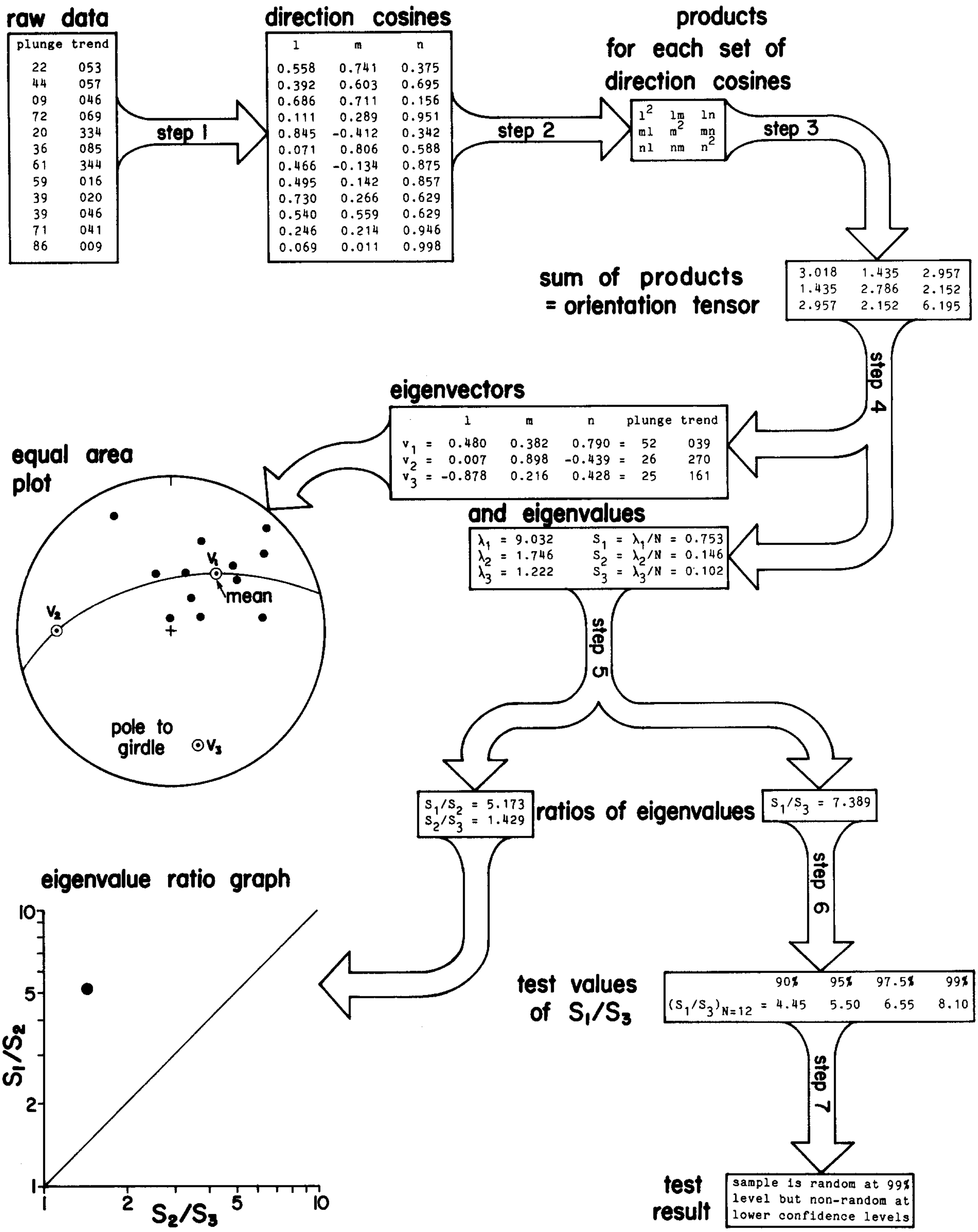

Fig. 10. Stepwise procedure for the S_1/S_3 test using real bedding pole data from part of the Batinah Mélange, Oman (Robertson & Woodcock 1983). See text for explanation.

(2) Compute the products for each direction-cosine set.
(3) Sum the products over the whole data sample to give the orientation tensor (equation 6 above).
(4) Compute the eigenvectors and eigenvalues of this matrix. (If the sample turns out to be non-random, the eigenvectors will give estimates of the cluster and girdle orientations in the sample.)
(5) Compute the eigenvalue ratios, particularly the ratio of the largest to smallest eigenvalue ($S_1/S_3 = \lambda_1/\lambda_3$). If the data are non-random they can usefully be represented as a point on an eigenvalue ratio graph, ln (S_1/S_2) vs ln (S_2/S_3).
(6) Refer to Fig. 9 or Table 1 and read off the critical S_1/S_3 value for the appropriate sample size and required confidence level. Note that for a small sample size a 95% confidence level is appropriate.

(7) If the computed value is *less* than the test value, the data sample cannot be distinguished from a random sample at this confidence level.

Steps 1–4 can be performed on a hand calculator (see algorithm by Cheeney, in press), but are best done by computer. We use a FORTRAN program STATIS (Woodcock 1973), listings of which can be obtained from us. Published routines to perform eigenvalue analysis are available (e.g. Davis 1973, pp. 166–167) and most computer systems have standard routines for deriving eigenvalues and eigenvectors of a matrix. Given these facilities, the S_1/S_3 test for randomness is very rapid, and arises naturally out of the now standard eigenvalue analysis of orientation data (Woodcock 1973, 1977, Nuttall & Cooper 1978, Mancktelow 1981, Cheeney in press).

DISCUSSION

Comparison of tests: Monte-Carlo samples

The random sampling program RANSACK outputs for each sample the eigenvalues needed for our S_1/S_3 test and for the Mardia and Anderson & Stephens tests. It also carries out the cell tests of Winchell and Dudley *et al.* and outputs a yes/no result. The results of all tests are compared on Fig. 11 for 95 and 99% confidence levels. A test which on average gives similar results to the S_1/S_3 test would, for every sample size in Fig. 11(a), class exactly 5% of samples as significant at the 95% level and exactly 1% at the 99% level. All tests depart from this ideal similarity. None show a strong correlation of performance with sample size (Fig. 11a) and therefore the results can be summarized on the histogram in Fig. 11(b).

The Mardia and Anderson & Stephens tests show the closest match to the S_1/S_3 test, probably because they are also based on eigenvalues. However they tend to class slightly more samples as significant. The Dudley *et al.* test gives different results for raw data and for data rotated so that the sample mean or girdle pole is at the net centre. The test on rotated data predicts fewer significant samples than the S_1/S_3 test. The Winchell test classes far too many samples as significant.

Comparison of tests: real field data

The various randomness tests have also been applied to 20 sets of real field data. All these sets appear close to random by visual inspection on an equal-area net. The results (Fig. 11c) confirm the relative bias of the tests established on the Monte-Carlo samples: the Mardia and Anderson & Stephens tests give results comparable with the S_1/S_3 test: the Winchell test classes too many samples as significant and the Dudley *et al.* test too few.

The majority of real data sets come from the following two areas.

(a) The Mamonia Complex, SW Cyprus (Robertson & Woodcock 1979): bedding pole data from non-metamorphic sedimentary sequences deformed at a shallow structural level.

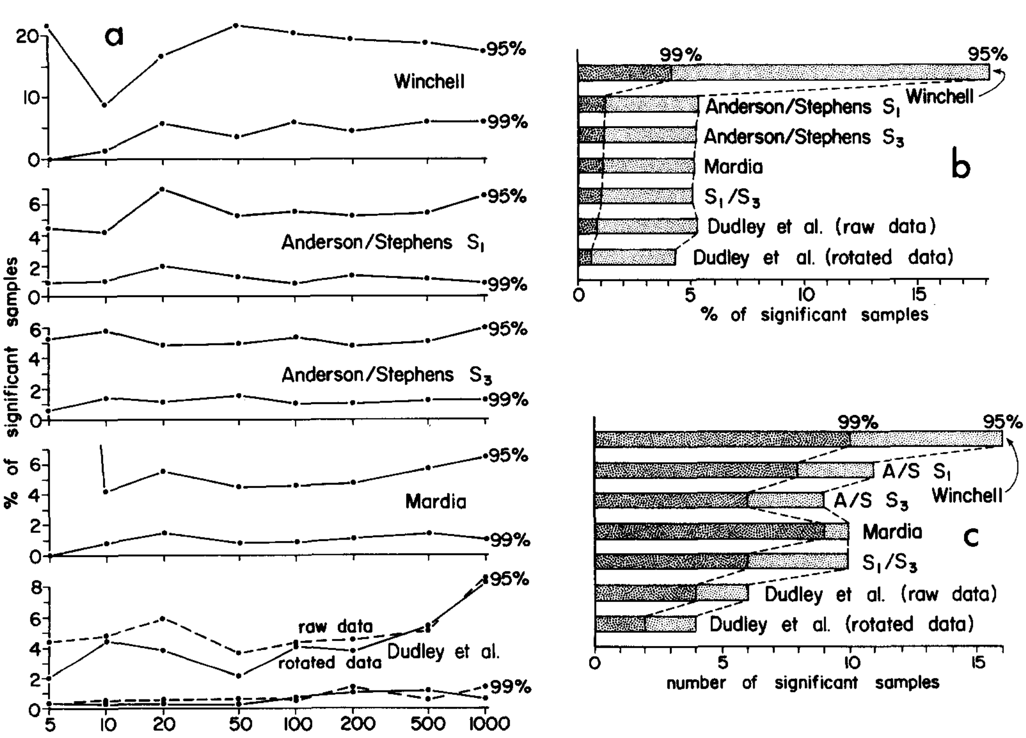

Fig. 11. The number of samples classed as significant by various tests at 95 and 99% confidence levels, (a) as a function of sample size (based on 1000 Monte-Carlo samples for each size indicated), (b) averaged over all 8000 Monte-Carlo samples and (c) for 20 real data samples (see text for discussion).

(b) The Batinah melange, Oman (Robertson & Woodcock 1983): bedding data from an olistostrome and slide-block mélange of ophiolitic and sedimentary debris.

We have also applied the test to other mélange units, to slump fold hinge lines, and to joints in an igneous body and a conglomerate. These initial applications give some idea of the range of field geological situations in which near-random data occur.

Sampling and sample shape

Any tests for randomness in orientation data depend on unbiased sampling of data in the field. The appropriate sampling plan should be carefully considered (e.g. Davis 1973, Cheeney in press).

One problem in applying the S_1/S_3 test is that the eigenvector method cannot cope adequately with certain types of multimodal data (Woodcock 1977). For this reason the test, as with most other tests reviewed here, could wrongly return a random result from a dataset consisting of several individually significant modes or superimposed samples. This problem frequently arises with joint data and structures in multiply deformed areas. For this reason we recommend inspecting the form of the data on an equal-area plot before accepting the results of any randomness test. If several modes appear to be present then some independent test for multimodality (e.g. Bailey 1975) should be made, together with some attempt to separate data from the various modes (Kohlbeck & Scheidegger 1977) before proceeding further.

ADVANTAGES OF THE S_1/S_3 TEST

The comparisons above suggest that only the Winchell randomness test gives grossly misleading results. Other available tests give results approximately consistent with our Monte-Carlo tests. We suggest the following advantages for the S_1/S_3 test over these other tests.

(1) It is rotationally invariant, unlike the various cell tests.

(2) It is independent of the 'shape' of the sample. The two Anderson & Stephens methods test against the hypotheses of a uniaxial cluster and a uniaxial girdle, respectively. Most randomly generated samples of a uniform distribution fall between these two extremes (Fig. 6).

(3) S_1/S_3 is a natural 'strength' parameter, in that lines of equal S_1/S_3 tend to delimit fields of equal point density on the ratio plot of the Monte-Carlo samples (Fig. 6).

(4) The S_1/S_3 statistic is simply calculated during the now widely used eigenvalue method of orientation data analysis.

(5) The test graph (Fig. 9) has proved to be a rapid and practical visual method. Table 1 can be used for more precise testing.

Acknowledgements—We thank Bill Owens who suggested the approach for producing a uniform distribution, and Adele Prouse for drafting the figures. The example data from Oman were collected by N.H.W. jointly with Alastair Robertson.

REFERENCES

Anderson, M. A. & Stephens, M. A. 1972. Tests for randomness of directions against equatorial and bimodal alternatives. *Biometrika* **59**, 613–621.

Bailey, A. I. 1975. A method of analysing polymodal distributions in orientation data. *J. Int. Ass. math. Geol.* **7**, 285–293.

Chayes, F. 1949. Statistical analysis of three-dimensional fabric diagrams. In: *Structural Petrology of Deformed Rocks* (edited by Fairbairn, H. W.). Addison Wesley, Reading, MA, U.S.A., 297–326.

Cobbold, P. R. & Gapais, D. 1979, Specification of fabric shapes using an eigenvalue method: Discussion. *Bull. geol. Soc. Am.* **90**, 310–312.

Cheeney, R. F. in press. *Statistical Methods in Geology for Field and Laboratory Decisions.* George, Allen & Unwin, London.

Davis, J. C. 1973. *Statistics and Data Analysis in Geology.* Wiley, New York.

Dudley, R. M., Perkins, P. C. & Gine, E. 1975. Statistical tests for preferred orientation. *J. Geol.* **83**, 685–705.

Fisher, R. A. 1953. Dispersion on a sphere. *Proc. R. Soc. Lond.* **A217**, 295–305.

Flinn, D. 1958. On tests of significance of preferred orientation in three-dimensional diagrams. *J. Geol.* **66**, 526–539.

Flinn, D. 1962. On folding during three-dimensional progressive deformation. *Q. Jl geol. Soc. Lond.* **118**, 385–433.

Flinn, D. 1978. Construction and computation of three-dimensional progressive deformations. *J. geol. Soc. Lond.* **135**, 291–306.

Harvey, P. K. & Ferguson, C. C. 1978. A computer simulation approach to textural interpretation in crystalline rocks. In: *Recent Advances in Geomathematics* (edited by Merriam, D. F.). Pergamon, Oxford, 201–232.

Harvey, P. K. & Laxton, R. R. 1980. The estimation of finite strain from the orientation of passively deformed linear markers: eigenvalue relationships. *Tectonophysics* **70**, 285–307.

Kohlbeck, F. & Scheidegger, A. E. 1977. On the theory of the evaluation of joint orientation measurements. *Rock Mechanics* **9**, 9–25.

Mancktelow, N. S. 1981. A least-squares method for determining the best-fit point maximum, great-circle and small-circle to non-directional orientation data. *J. Int. Ass. math. Geol.* **13**, 507–521.

Mardia, K. V. 1972. *Statistics of Directional Data.* Academic Press, London.

Mark, D. M. 1973. Analysis of axial orientation data, including till fabrics. *Bull. geol. Soc. Am.* **84**, 1369–1374.

Mark, D. M. 1974. On the interpretation of till fabrics. *Geology* **2**, 101–104.

Nuttall, D. J. H. & Cooper, M. A. 1978. Computer programs for the analysis and presentation of orientation data. *J. geol. Soc. Lond.* **135**, 243–244.

Robertson, A. H. F. & Woodcock, N. H. 1979. The Mamonia Complex, southwest Cyprus; the evolution and emplacement of a Mesozoic continental margin. *Bull. geol. Soc. Am.* **90**, 651–665.

Robertson, A. H. F. & Woodcock, N. H. 1983. Genesis of the Batinah melange above the Semail ophiolite, Oman. *J. Struct. Geol.* **5**, 1–17.

Scheidegger, A. E. 1965. On the statistics of the orientation of bedding planes, grain axes and similar sedimentological data. *Prof. Pap. U.S. geol. Surv.* **525C**, 164–167.

Starkey, J. 1977. The contouring of orientation data represented in spherical projection. *Can. J. Earth Sci.* **14**, 268–277.

Wallbrecher, E. 1979. Methodem zum quantitativen Vergleich von Regelungsgraden und -formen strukturgeologischer Datenmengen mit Hilfe von Vectorstatistik und Eigenvert-Analyse. *Neues Jb. Geol. Paläont. Mh.* **159**, 113–149.

Watson, G. S. 1966. The statistics of orientation data. *J. Geol.* **74**, 786–797.

Williams, G. D. & Spray, J. G. 1979. Non-cylindrical, flexural slip folding in the Ardwell Flags—A statistical approach. *Tectonophysics* **58**, 269–277.

Woodcock, N. H. 1973. The structure of the slump sheets in the Ludlow Series of east central Wales. Ph.D thesis, Univ. of London, England.

Woodcock, N. H. 197. Specification of fabric shapes using an eigenvalue method. *Bull. geol. Soc. Am.* **88**, 1231–1236.